

## **Velestino 3 - Mati**

### **Archaeological Background**

Magoula Velestino 3 or Mati, is an oval shaped hill inhabited from Early until Middle Neolithic and on Early Bronze Age. There are also several finds scattered on the surface that indicate some human appearance during later historical periods too. The site is divided in several different levels of high, probably because of the different cultivated fields although it is possible that these are the remnants of ancient structures and formation of the area.

### **Satellite Remote Sensing and Historical Aerial Photography Survey**

A GeoEye-1 image from 4 May 2010 was used for satellite remote sensing at Velestino 3 (Mati) (Figure 1). The satellite image has an off-nadir angle of  $9.9^\circ$  and a ground sampling distance (GSD) of 0.50 m (panchromatic) and 1.81 m (multispectral). In addition to the satellite imagery, an aerial photograph from 26 August 1960 was used with a scale of 1:15,000 (Figure 2).

The environment around Velestino 3 (Mati) is level agricultural land with some rolling hills that rise gradually toward the west. The town of Velestino stands only 1 km to the southwest. The eastern topography beyond the National Road (800 m away) rises more sharply toward the foothills of Mt. Pelion. Various streams, irrigation channels, and roads leading to Volos pocket the terrain. There are some modern constructions, including large industrial installations especially toward the east. Several other prehistoric settlements are located in the same area. These include Nikonanou (1.4 km to the northeast), Velestino 4 (Visviki) (1.8 km to the east), and Magoula Bakalis (1.4 km to the southwest). The prehistoric tell is also 700 m away from the extra-mural sanctuary of Zeus Thavlios, which was an important cult site for the nearby classical Greek city of Pherai (now located beneath modern Velestino). Cultivation in the region is predominantly wheat and olives. Elevations around Velestino 3 (Mati) range from 80-90 masl.

The local environment and land use around Velestino 3 (Mati) have not undergone significant changes like the nearby prehistoric sites of Nikonanou and Velestino 4 (Visviki). Some field boundaries and field orientations are different in the 23 August 1960 aerial photograph than they appear in the 4 May 2010 GeoEye-1, but beyond this there are no large alterations or evidence of redirected rivers.

Satellite remote sensing within a 1 km radius around Velestino 3 (Mati) produced some interesting results (Figures 3-4). The majority of features correspond to palaeochannels (blue) associated with the rivers and streams that once pocketed the terrain, especially to the northwest of the tell. Some other anomalies relate to agricultural activity (brown), such as former field divisions and plow lines. A third category of anomalies is unclassified (yellow). The habitation mound appears as a circular surface anomaly 70 m in diameter in several feature enhancement indices (Figure 5). The evidence is not overwhelming, but it is enough to give a general impression of its basic form. One notices soil and vegetation stress even in RGB pansharped images, and these become more definite with PCA, IR/R, and MSAVI. Approximately 450 m south of Velestino 3 (Mati), anomaly 96 is a clear circular soil mark in an uncultivated field (Figure 6). The true color RGB image shows the feature as a darkened area around lighter soil. The distinctions are better with spectral filters, such as MSAVI. The diameter of anomaly 96 is

just less than 100 m. Noting the density of prehistoric mounds in the region, this feature may be a potential candidate for another (unknown) prehistoric settlement.

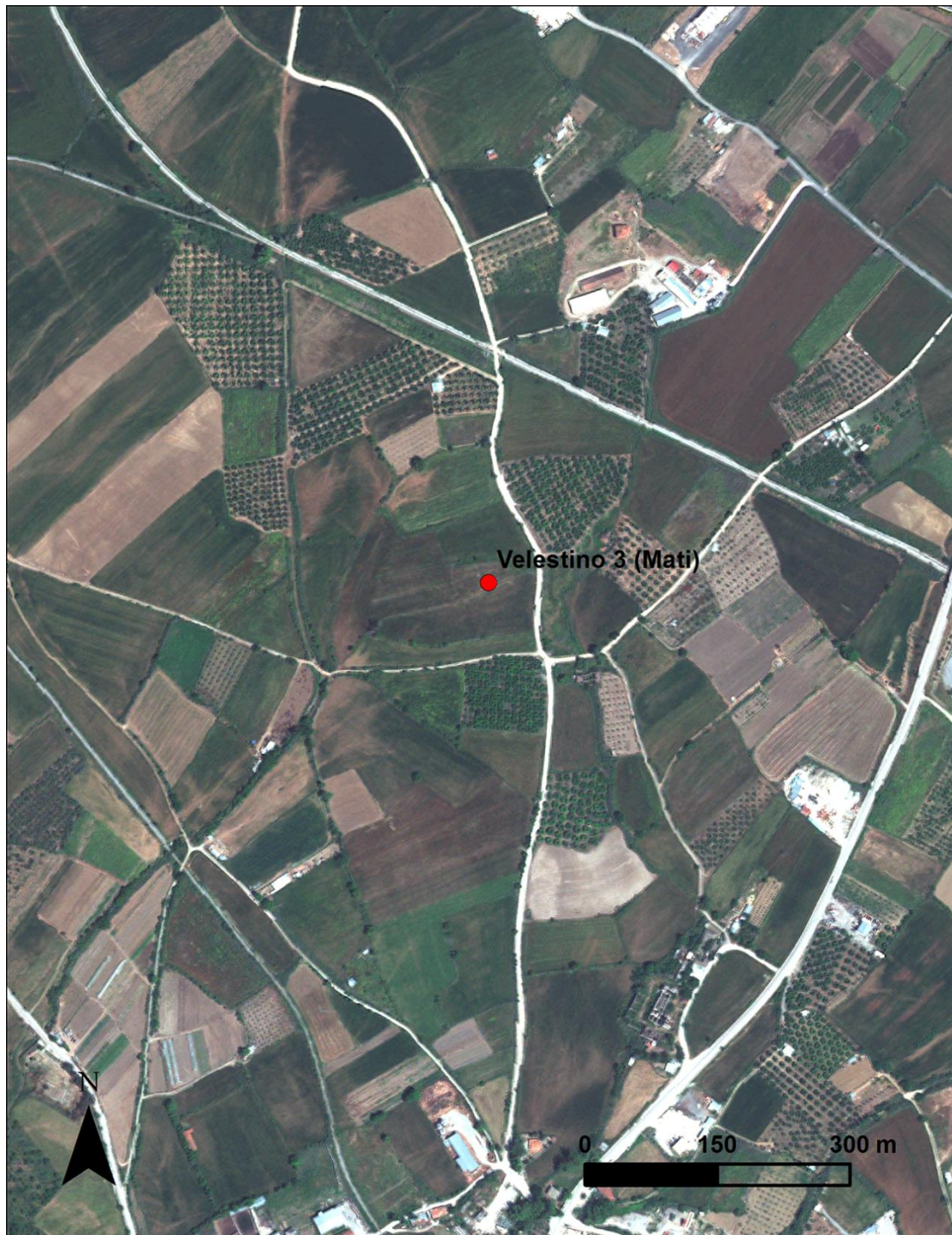


Figure 1: Velestino 3 (Mati) from a 4 May 2010 GeoEye-1 image



Figure 2: Velestino 4 (Mati) from an aerial photograph taken 26 August 1960

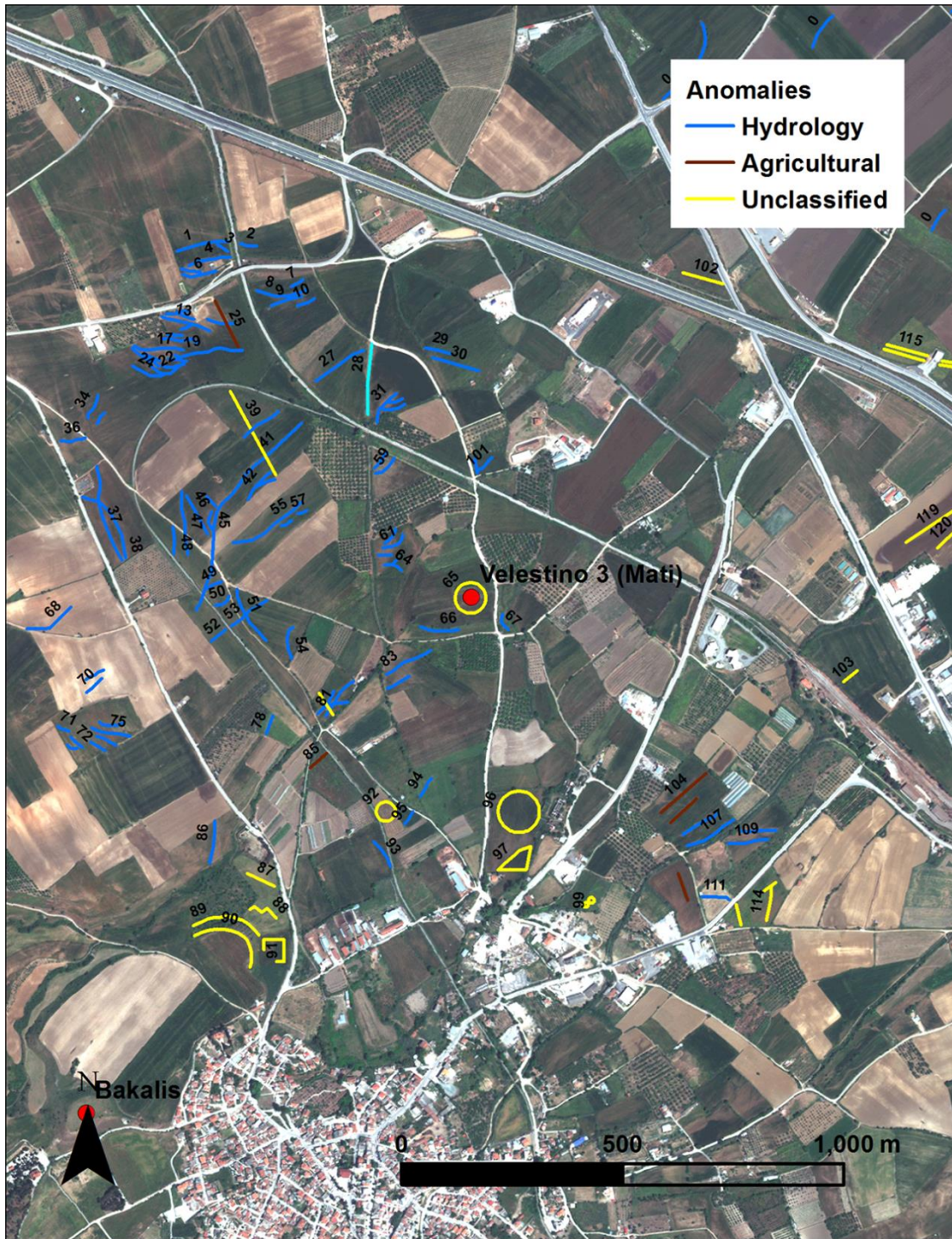


Figure 3: Surface anomalies from the 4 May 2010 GeoEye-1 image within a 1 km radius around Velestino 3 (Mati)



PCA



ARVI



Green NDVI



MSAVI



MSR



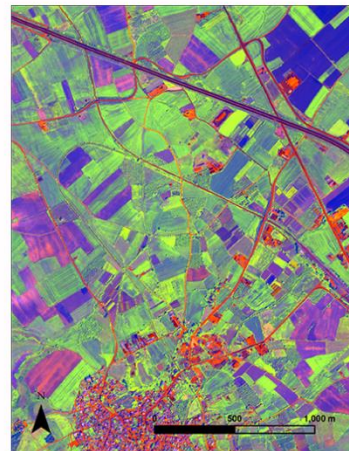
NDVI



Decorrelation Stretch



RGB to IHS



Tasseled Cap

Figure 4: Spectral filters and vegetation indices applied to the 4 May 2010 GeoEye-1 image around Velestino 3 (Mati)



Figure 5: IR/R of the 4 May 2010 GeoEye-1 image around Velestino 3 (Mati) showing a circular anomaly that mark the location of the prehistoric tell

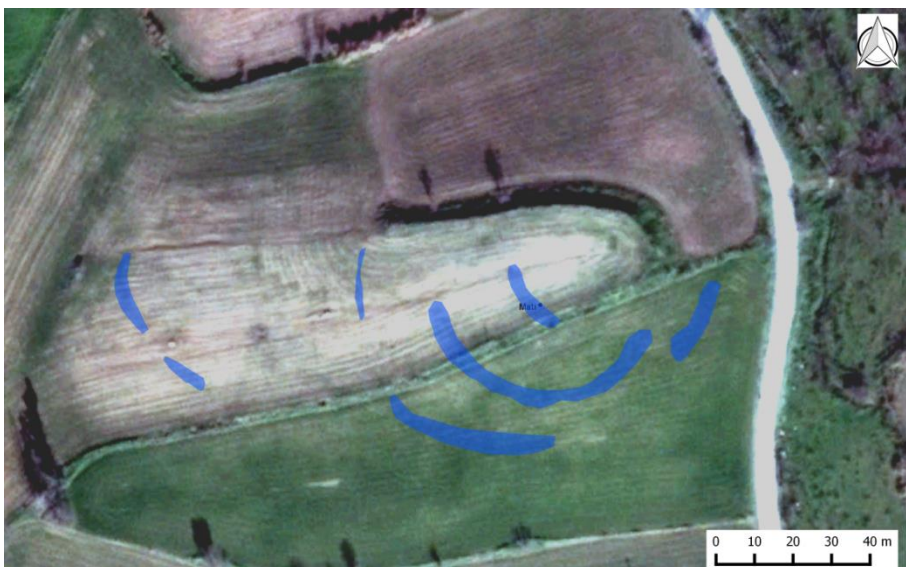


Figure 6: True color RGB (left) and MSAVI (right) of the 4 May 2010 GeoEye-1 image showing a circular anomaly (#96) 450 m south of V

#### Remotely Piloted Aircraft Systems (RPAS) Survey

The site of Velestino Mati has been photographed with all available cameras (GoPro, regular RGB and modified NIR), but no relevant trace could be identified during their analysis. Also the DEMs produced in photogrammetry didn't return any particular altimetric anomaly of interest.

The exam of the internet orthophotos instead gave some additional information to integrate with the results from geophysics. In particular, one image from DigitalGlobe (accessible through Google Earth) dated to January 23<sup>rd</sup> 2013, shows some circular traces –possibly ditches– that match and complete the geophysics.



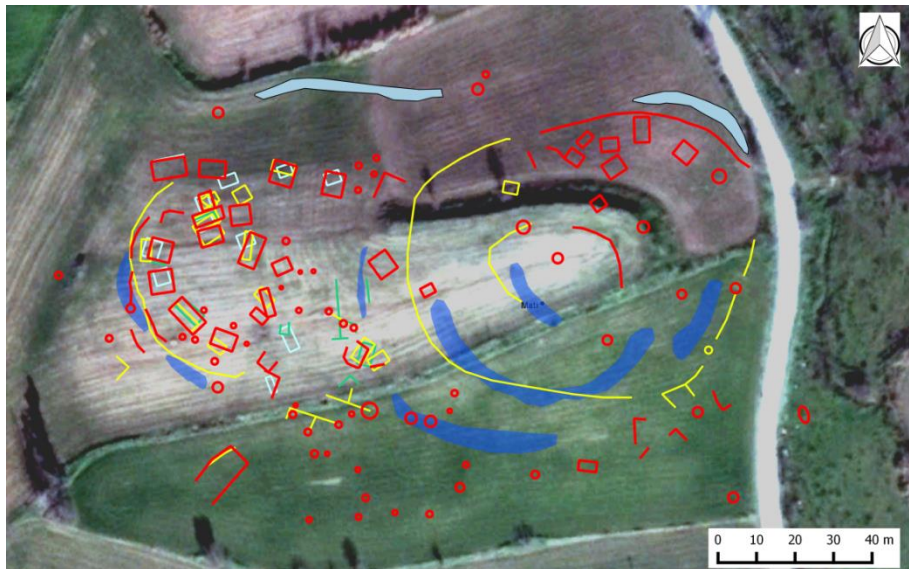


Figure 7: Orthophoto from DigitalGlobe with AerialPhotoInterpretation (light blue, top image) and geophysics.

## Geophysical Prospection

### Geomagnetic Survey

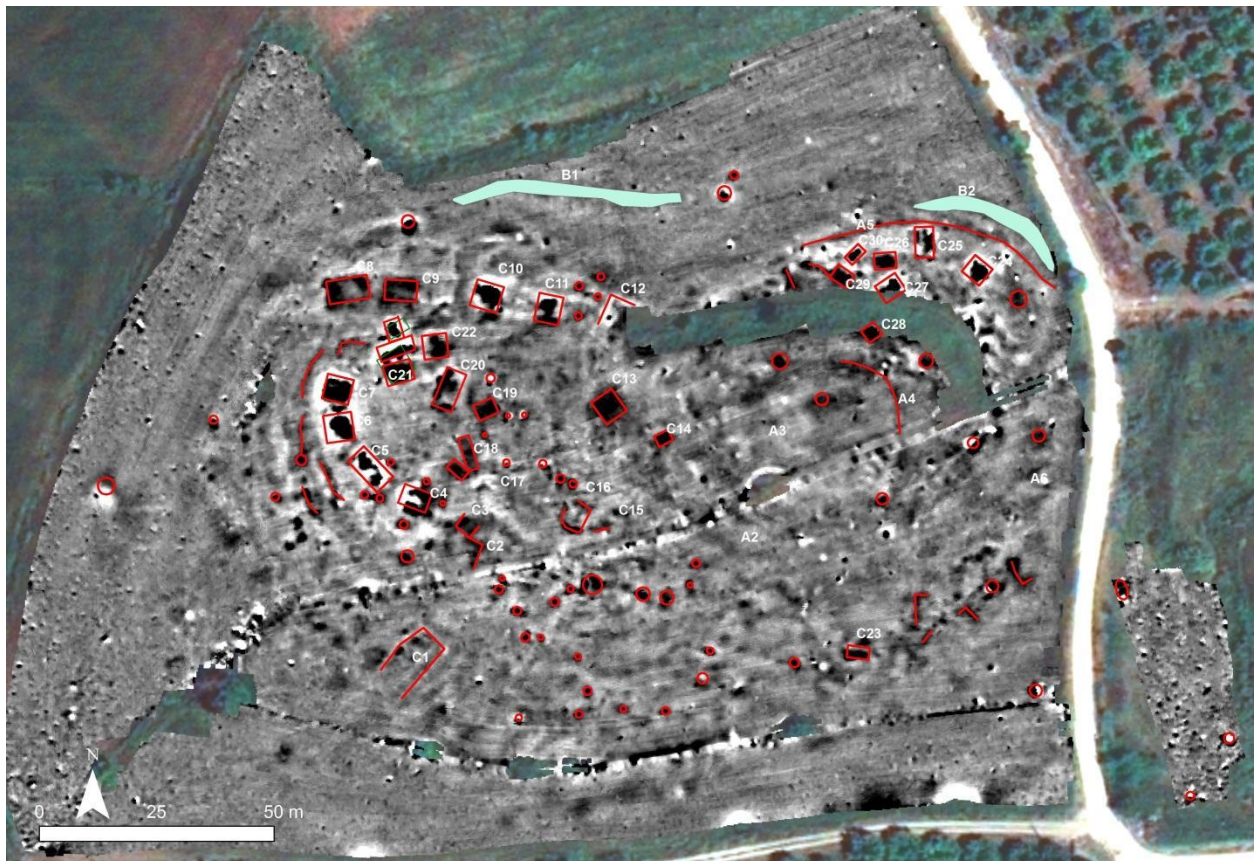


Figure 8: Geomagnetic results from Mati



Velestino 3 – Mati is a bean/ellipsoid shaped settlement with two apparent settlement cores, one to the east and one to the west. Overall, the settlement is characterized by a series of buildings to the north and a sharp division between anthropogenic-natural divisions to the south. The core at the west contains more documented features than the eastern core despite the fact that some data are missing in the east. The saddle contains two anomalies (C13 and C14) circular in shape and high in magnetic values. Especially, C13 has the potential to be a large pit, serving both east and west cores.

The western core has features aligned in a circular shape, leaving an open space at the center. The architectural elements present evidence for burning. To the north of this circular layout, we also observe a series of potential buildings (C8, C9, C10, and C11). It is possible that this alignment continues up until the eastern core. However, chunks of data are missing to secure this argument. In the eastern core, we observe, buildings are clustering to the northeast. Even if one takes into account the missing data, the eastern core is not established as well as the western one. Anomalies (C24-30) do not form a coherent layout, but rather cluster.

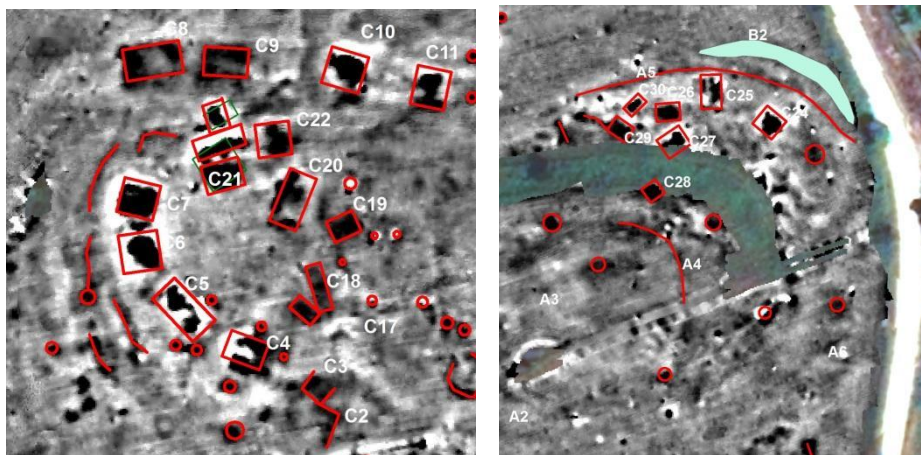


Figure 9: A geomagnetic focus on the western and eastern

cores of the settlement

### *Electromagnetic Induction Survey*

EM survey was done with the GEM2 from Geophex with a GPS positioning and with the CMD mini-explorer from GF Instruments. The use of both of these instruments presents the advantage to give valuable information for two depths of investigation and three geophysical parameters (for the susceptibility 1.6 meter for the GEM2 and 1.3 meter for the CMD min-explorer). Other depth of investigation are given by the CMD but the small offset between the coils give in this case a very low depth of investigation mainly disturbed by the soil heterogeneity. They are not presented here.

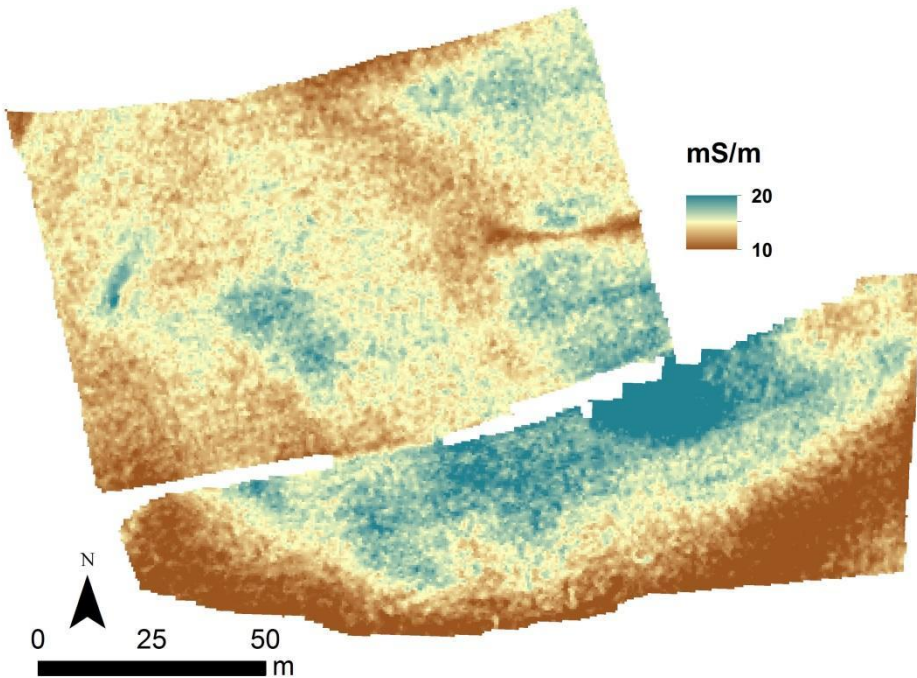


Figure 10: Electrical conductivity for the GEM2

On the electrical conductivity map we observe some global variation related to the variability of soil nature (Figure 10). On the south part of the map the result shows a clear distinction between the inside part and the outside part of the Neolithic settlement with a low conductivity for the outside part. This effect is probably involved by the nature of the archaeological sediment presenting higher clay content.

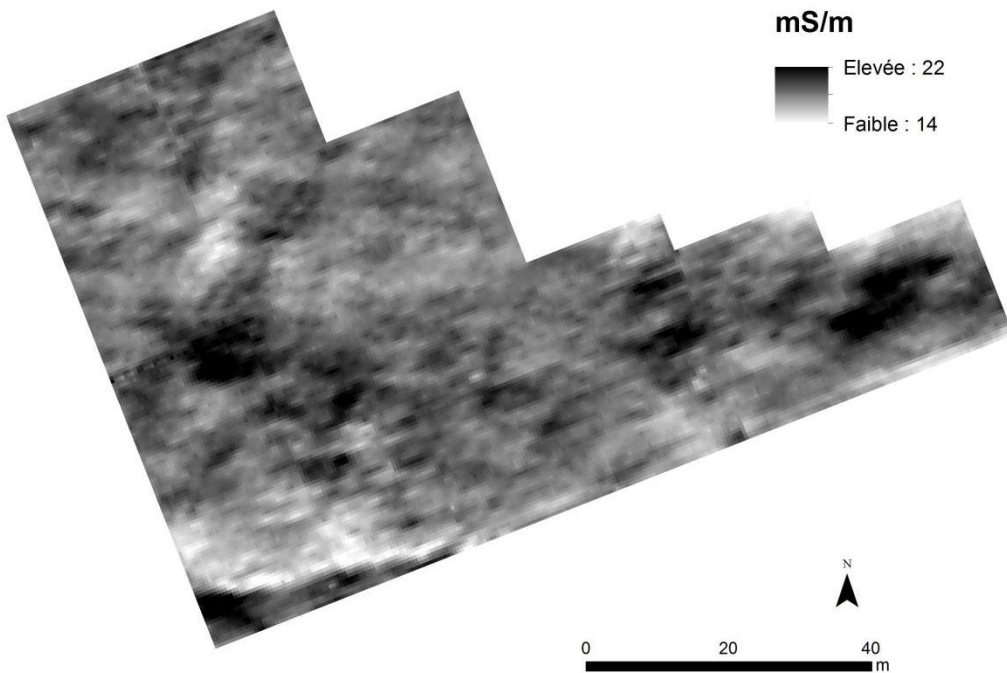


Figure 11: Electrical conductivity for the CMD Mini-explorer

For the CMD mini-explorer and for the largest coils separation (1.3 meter), the map of the electrical conductivity (Figure 11) is not clear as for the GEM-2. This is probably caused by a low conductivity of the topsoil. Some anomalies present a high value of conductivity. These anomalies are not directly related to the magnetic anomalies who are clearer in term of definition.

As usually in the context of the Neolithic settlement of Thessaly the magnetic susceptibility show the best EM result for the archaeological characterization (Figure 12). The main value of this dataset concerns the depth of investigation but also the detection of some magnetic layer (in brown). If the magnetic anomalies (resulting from the magnetic measurement) are not visible on the magnetic susceptibility we can conclude on a deeper feature, it the case for the C8, C9 C12 or C13 for example. Also in the area of C15 and C16 and in the south of these two anomalies we observe many high magnetic susceptibility anomalies (larger than the previous one). These ones correspond probably to a magnetic layer which is not detectable with the magnetic measurement. It explains also the presence of linear anomalies on the magnetic dataset corresponding to the border of this susceptible anomaly. It is also the case in the north part close to the C22 and C20 anomalies. Also the magnetic susceptibility coming from the GEM2 shows a large magnetic anomaly around the settlement which corresponds with the anomalies detected on the satellite images. The center part of this settlement presents a strong soil heterogeneity induced probably by a large number of archaeological structures.

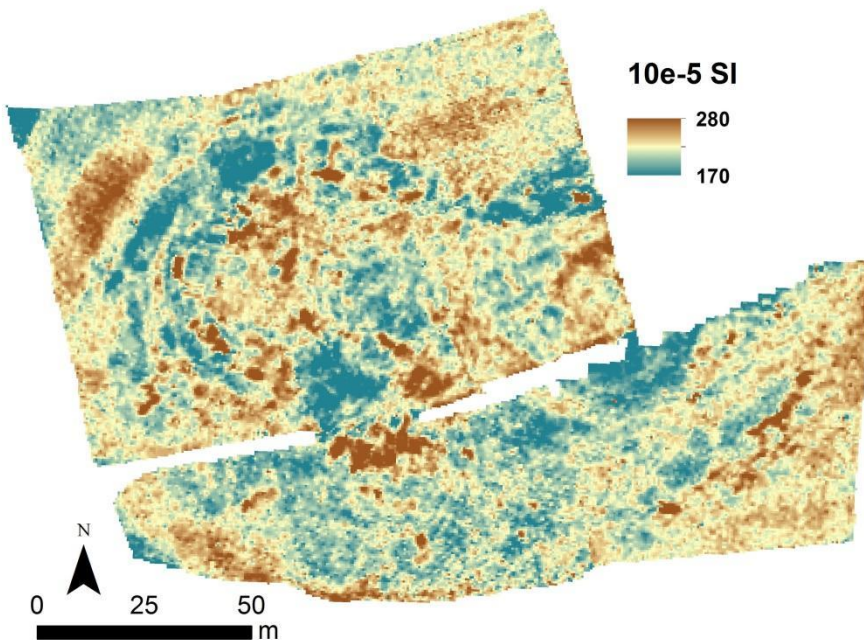


Figure 12: Magnetic susceptibility for the GEM2

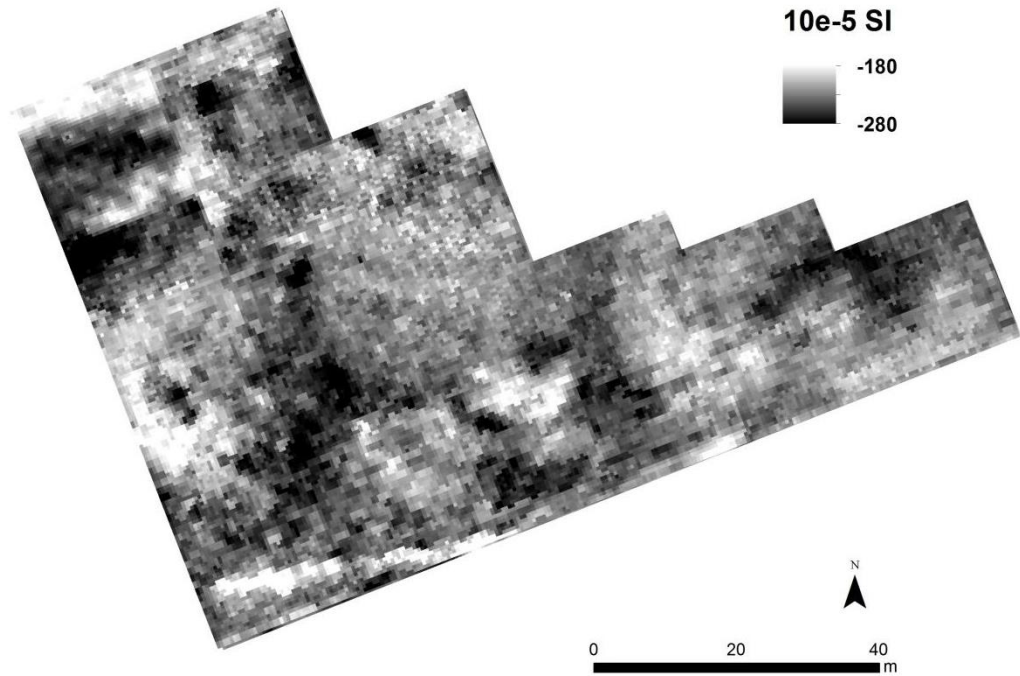


Figure 13: Magnetic susceptibility for the CMD

For the CMD Mini-explorer, the magnetic susceptibility are less clear (Figure 13). Some strong anomalies are still visible but the map present also a strong level of noise. Here we observe the existence of features closer to the ground surface than for the GEM2 magnetic susceptibility map. The value in term of archaeological characterization is relatively poor.

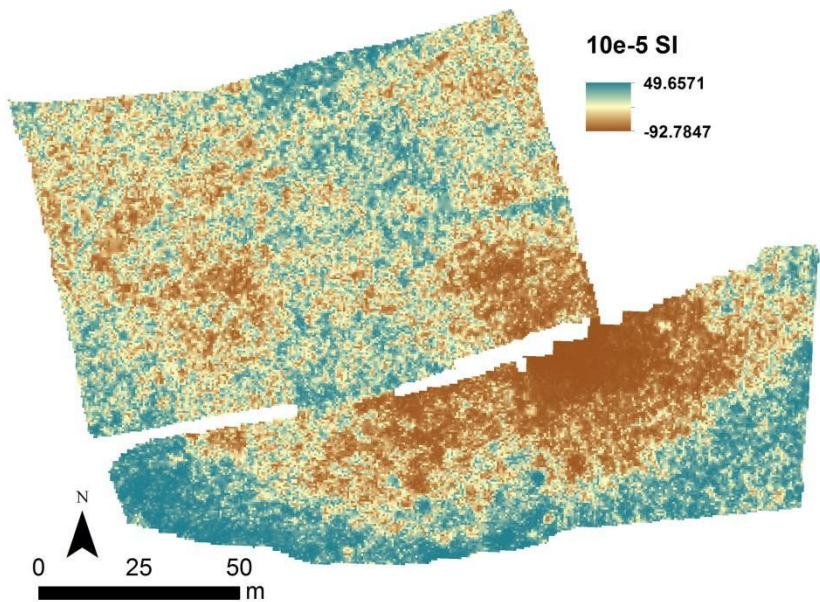


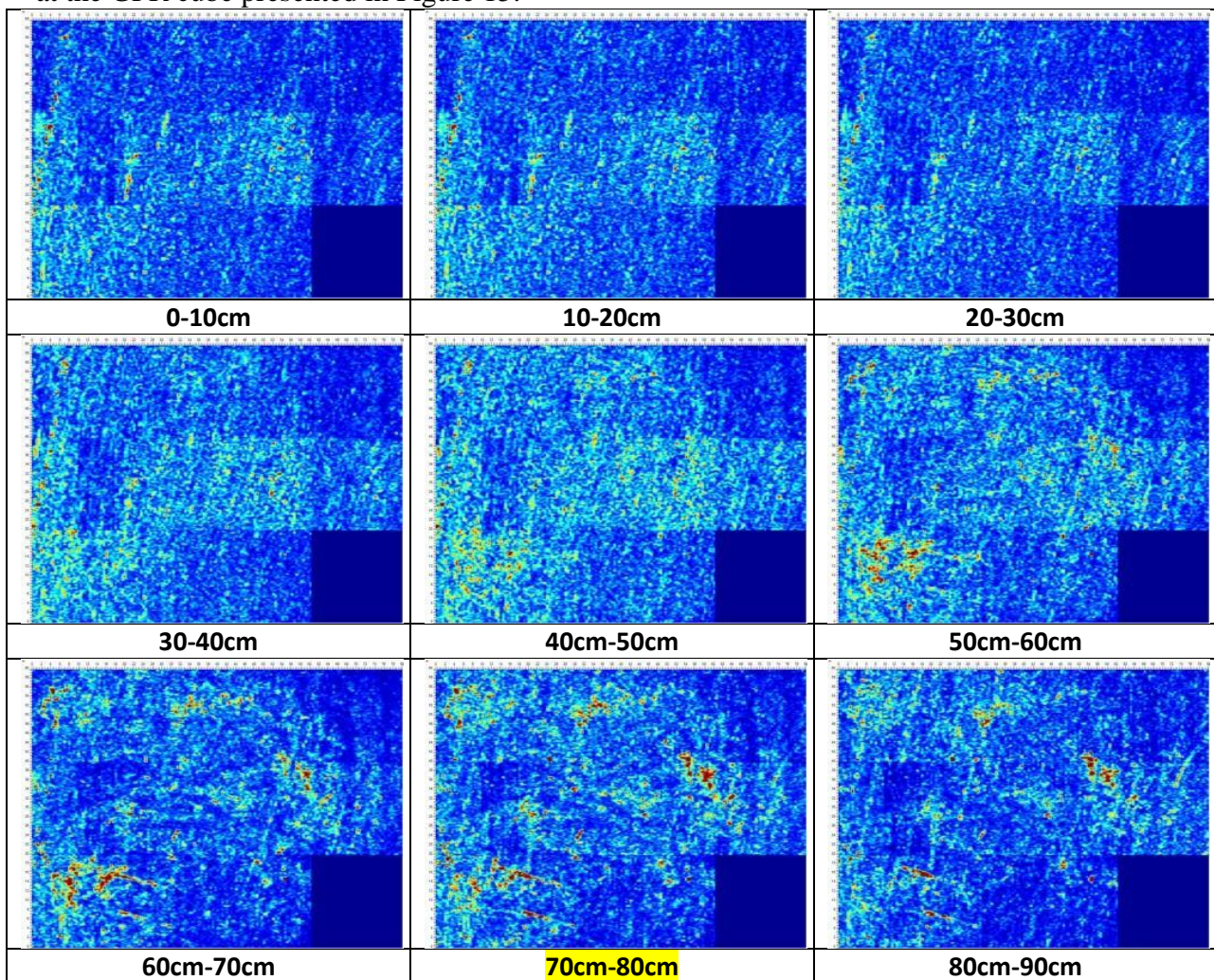
Figure 14: Magnetic viscosity for the GEM2

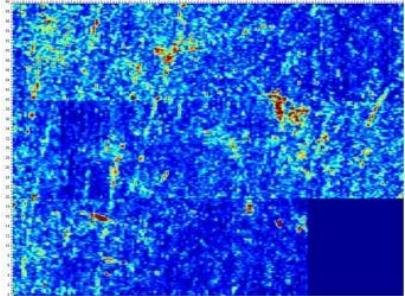
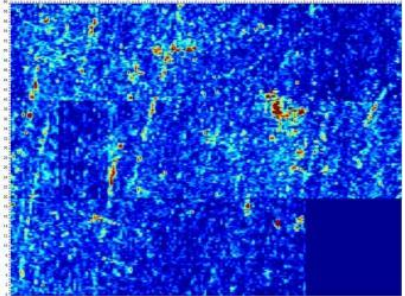
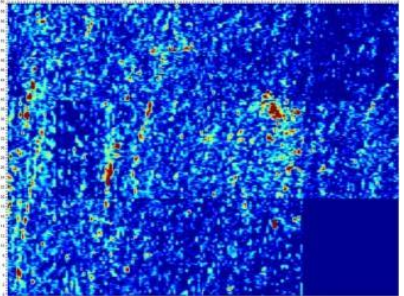
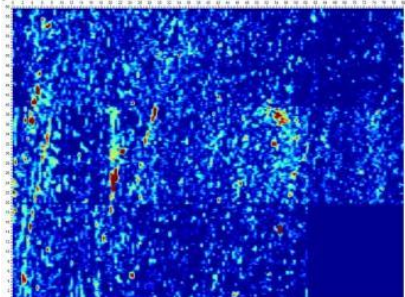
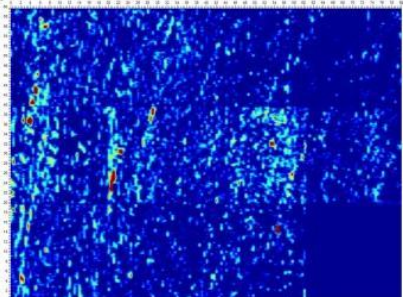
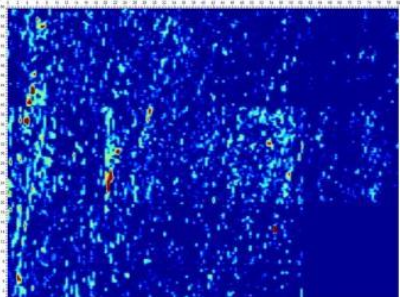
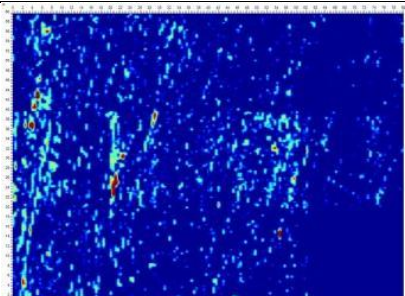
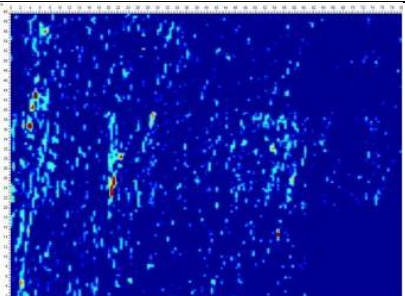
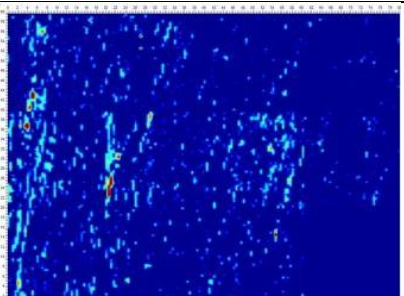
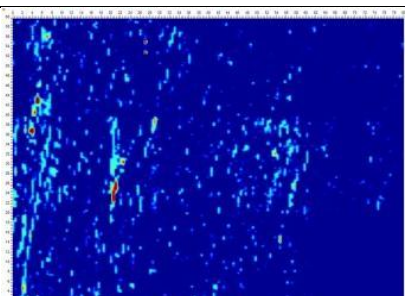
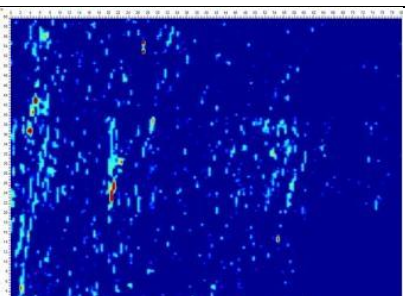
The map of magnetic viscosity results mainly from a bad processing of the magnetic viscosity (Figure 14). In this context, the magnetic viscosity shows the same distribution on the map than the electrical conductivity. It probably comes from a poor characterization of the electrical conductivity in this area. Nevertheless it presents also clearly the distinction between the inside and the outside part of the settlement.

### *Ground Penetrating Radar Survey*

The total area covered at Velestino Mati with Noggin Plus Smart Cart is 4400m<sup>2</sup> and consists of 9 grids. The survey grids were set according to the pottery distribution on the flat area at the top of the settlement. The data collected were processed as follows: Trace reposition, Repick first break (10%), Dewow, Background average subtraction, Lowpass filter (f=50.0 % Nyquist), Highpass filter (f=30 % Nyquist). The resulting slices are presented in Table 1.

The results are noisy due to rocky terrain and the modern cultivation. The GPR signal's presents high attenuation returning no useful information below 100cm, indicating rich-clay environment. The most interesting anomalies that are more likely to be related with buried structures appear within the range 60 to 90cm below the surface. These anomalies are also shown along with noise at the GPR cube presented in Figure 15.



		
<b>90cm-100cm</b>	<b>100cm-110cm</b>	<b>110cm-120cm</b>
		
<b>120cm-130cm</b>	<b>130cm-140cm</b>	<b>140cm-150cm</b>
		
<b>150cm-160cm</b>	<b>160cm-170cm</b>	<b>170cm-180cm</b>
		<p>Table 1: GPR depth slices for the grids with labeled as VEL4 to VEL6 and VEL8 to VEL16, at Velestino Mati with 10cm thickness.</p>
<b>180cm-190cm</b>	<b>190cm-200cm</b>	

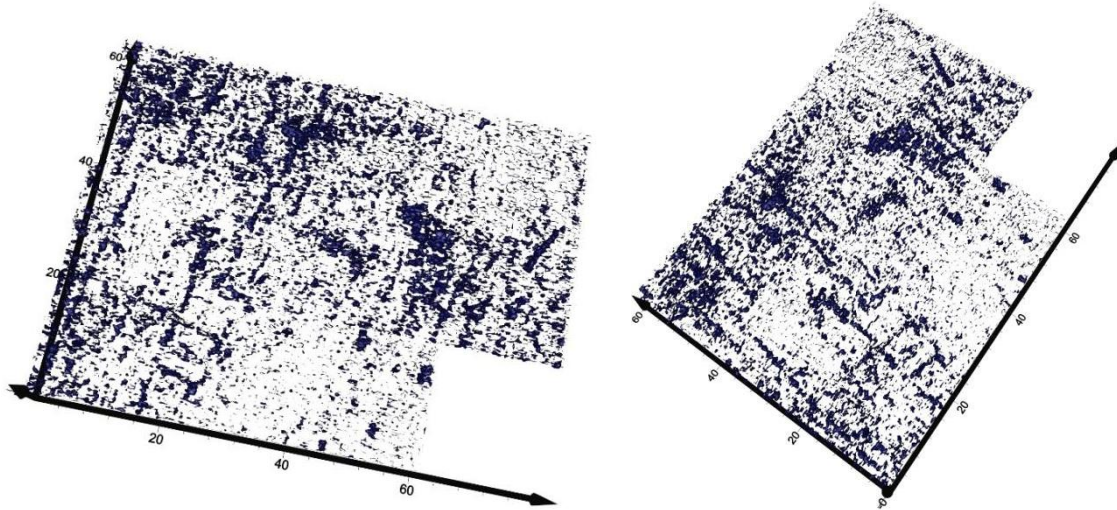


Figure 15: Different perspectives of the GPR 3D cube as occurred from the collected lines at Velestino Mati.

Figure 16 presents a representative GPR slice that describes the strongest anomalies at 70-80cm depth. A few of them were also identified in the magnetic results as well. Starting with the anomaly C5, it extends from 60 and up to 110cm and presents high amplitudes and irregular shape. Taking into account the magnetic anomaly appeared in the same position, the reflector is most likely a demolished structure. Similar to C5 are the anomalies described by C21, which are also identified as demolished structures. The linear anomaly C9 (Figure 16b) appears within the range 80-110cm depth and is related with the southernmost wall of the structure that is clearly visible on the magnetic results. Another structural fragment identified is described by C7 that is shown up as scatter anomalies of medium intensity but seems to follow the corresponding magnetic anomaly that is identified as a house. C15 and C17 also describe scatter anomalies of high amplitudes that form rectangular indicating structural remains and are not shown as clear in the magnetic results. Last, for the anomaly C16 two assumptions can be consider; the first is to be related with structural remains of a larger complex that has two parallel walls along the N-S direction and is divided into rooms while the second is to be structural remains of two individual buildings with the same orientation. Although it presents very strong amplitudes and clear linearity in GPR slices it wasn't detect with the rest of the geophysical methods applied. This indicates a structure(s) either of different building material than the rest identified or different destruction conditions e.g. intact to fire.

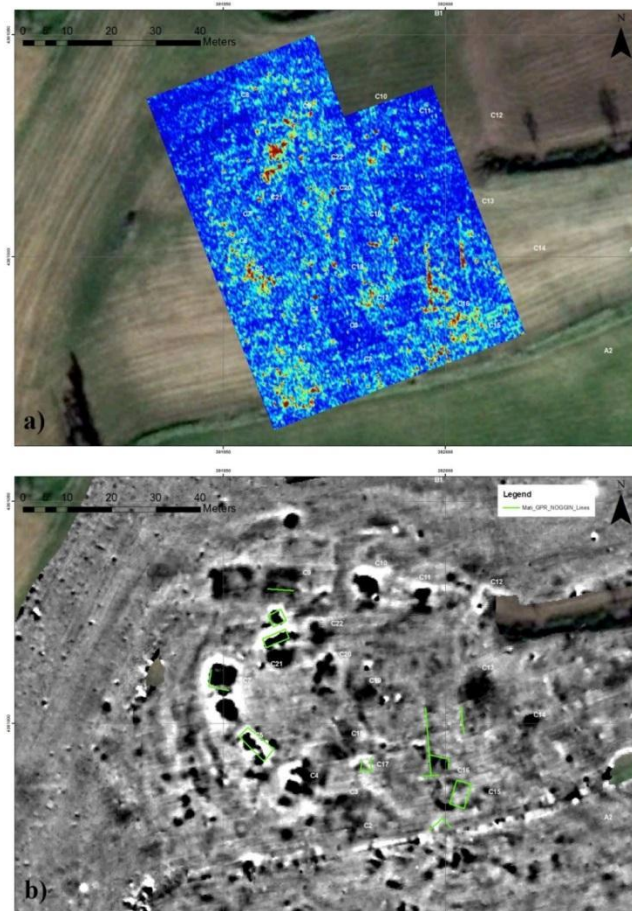


Figure 16: GPR results from the area of Velestino Mati, where a) is the georeferenced GPR slice at 70-80cm depth while in b) the identified anomalies are outlined with green color and are superimposed in the magnetic results for better comparison.

### *Resistance Survey*

Electrical resistivity data from Velestino Mati reveal significant details with respect to the use of space in the settlement (Figure 17). First, two settlement cores (as evident in the magnetic data) are also visible in the resistivity data with low readings. Especially, in the east side the boundary of this core is clearly defined, revealing the fact that east core was as large as the west core—an additional information on top of the magnetic data. However, these low resistivity areas possibly indicate preferential absence of the built environment. This evidence is available after evaluating resistivity data in comparison to the magnetic data where buildings in the magnetics are revealed as high resistance anomalies in the latter and magnetically homogenous areas appear as low resistivity areas. Furthermore, we have evidence of such buildings at the northeast edges of the survey area.

Linear anomalies with low resistivity values extending from these cores may be considered as ditches, retaining moisture hence increasing conductivity. The resolution of the survey does not permit to make further claims on potential single buildings. In the data, we also observe highly resistive areas scattered in the north and in high concentrations in the south of survey area. These anomalies nicely overlap with magnetic anomalies and provide further proof for structural elements. However, in addition to the magnetics, resistivity data suggests some “linear-arching”



anomalies in between settlement cores. Disregarding the high resistivity areas to the south of the survey area and considering the convexity towards the east these linear anomalies may represent built enclosures around the eastern core rather than the western core.

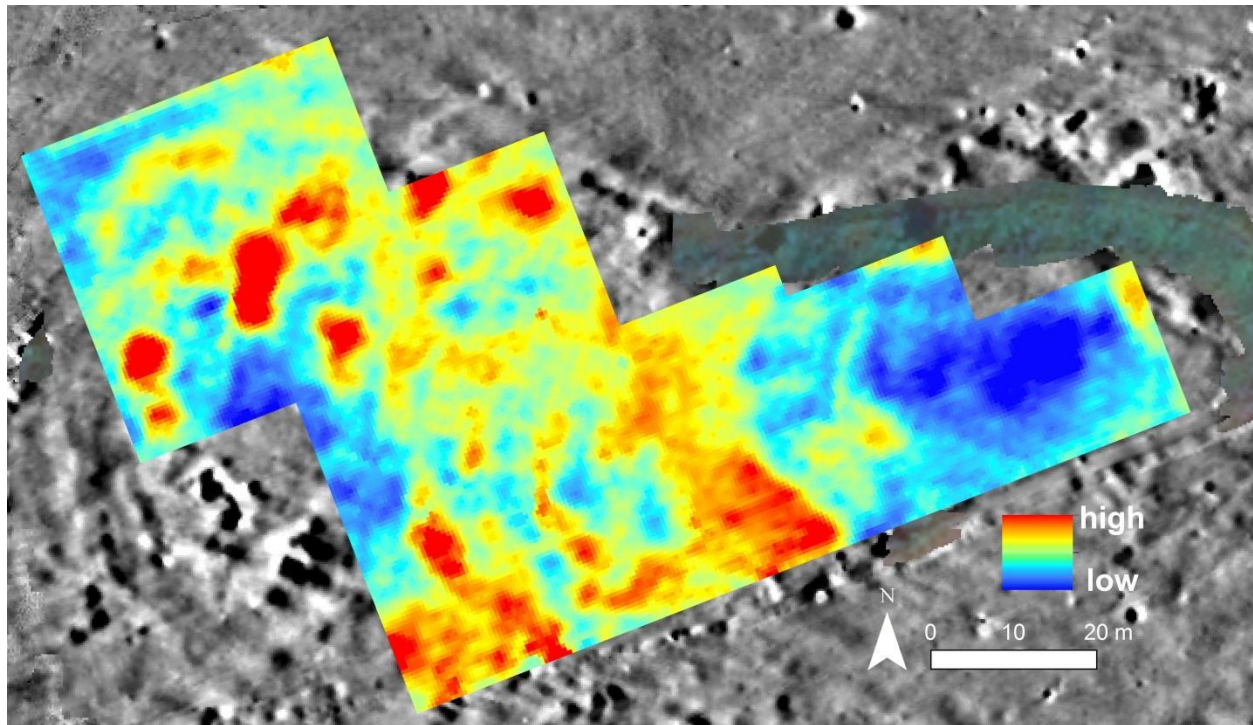


Figure 17: Resistance survey results from Velestino Mati

### Integration of Results

Magoula Velestino 3 - Mati is located about 1Km to the north of the town of Velestino and about 200m south of the railway line of Kalampakas-Volos. The shape of the magoula is oval with dimensions about 180x100m and it rises about 10m from the lower surrounding fields. The abundant surface material from the site indicates a continuous habitation from the Early Neolithic to the Bronze Age. Geophysical research was carried out using magnetic (SENSYS), soil conductivity/magnetic susceptibility (EM GEM2 and CMD), soil resistance (1m Twin probe array) and GPR (Noggin Plus 250MHz) techniques. The largest coverage of the site was accomplished through the magnetic survey that covered not only the magoula itself but also the surrounding fields around it and across the road to the east of the magoula. The latter region did not produce any significant results, and even the surrounding fields were almost empty of any geophysical indications.

The magnetic measurements were illuminating in terms of the anomalies that exist at the top and the sides of the magoula. A number of targets have been identified to the west and east section of it, most of which suggest the existence of burnt daub-made structures. This has also been confirmed from fragments of burnt daub that have been found during the survey to the NE slopes of the magoula. A cluster of structures (C2-C7 & C17-C22) aligned in a circular way constitutes the core of the habitation to the west. The houses are rectangular and some of them elongated and expand in an area of about 35x45m leaving and empty unbuilt space at the center. A few of the houses, such as C21, seem to consist of a series of compartments. Further to the north,

another strip of structures (C8-C12) appears expanding towards the northern slopes of the magoula. More structures are suggested as we move towards the east section of the magoula, with C13-C16 being located to the center of it. Even if there are some vague anomalies to the rest of the area, it is hard to conclude about the existence of other structural remains until we reach the NE side of the magoula, where again we have strong magnetic signals from another zone of structures (C25-C30) oriented along the NE slope of it. It is significant to mention that most of the above mentioned houses have been verified by the rest of the techniques: C2, C6, C7, C9, C10, C11, C17 and C20 with soil resistance techniques, C5, C7, C15, C16, C17 and C21 with the GPR and C4, C5, C7, C10, C15, C16, C18, C20, C21 and C22 with the EM magnetic susceptibility methods. Furthermore, GPR slices indicated that the cultural layers extend about 70cm below the current surface of the magoula. A few more isolated features are indicated to the south: C23 which is probably correlated with a structure and C1 which is most likely caused by modern interventions to the site (illegal excavations?).

The distinct oval shape of the magoula, clearly differentiated from the circular shape of most of the magoules in Thessaly, and the clustering of the suggested structures to the west and the east parts of the magoula, may indicate that we are dealing with two neighborhoods or two neighboring magoulas. This is also supported by the magnetic and EM magnetic susceptibility measurements that provide further evidence of two separate enclosures for the west and east sections of the site. To the west side of the settlement it is the western wall which is mostly well preserved. In contrast, to the east section it is possible to distinguish two enclosures, most probably fortification walls, which encircle the east neighborhood. Most of the houses to the east are also clustered between the two enclosures.

Even if Velestino 3 – Mati is located within a flooding region due its vicinity to Lake Karla, the large elevation of the magoula could indeed make any use of ditches around it unnecessary. A few features that are indicated to the north close to the base of the magoula may indicate the residues of past flooding episodes that left unaffected the occupants of the magoula.

Figure 18: The distribution of anomalies over geomagnetic results

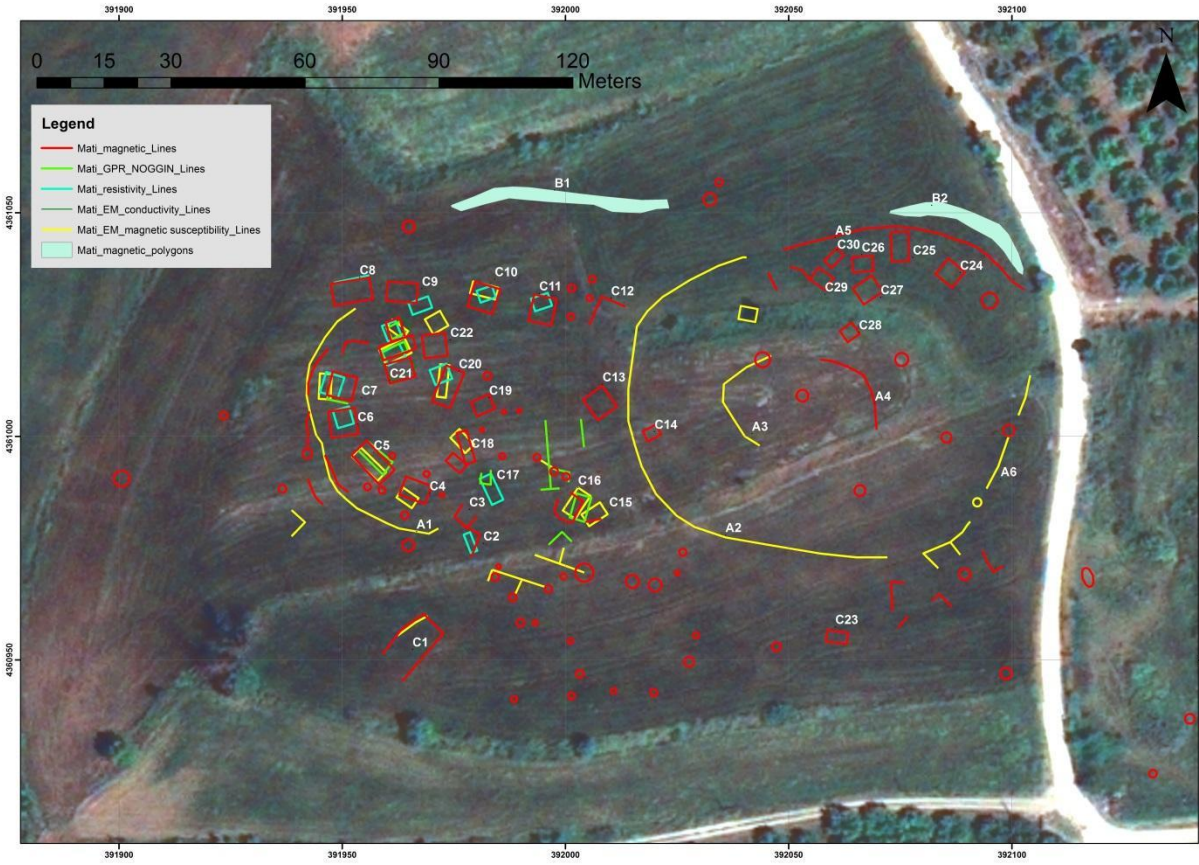
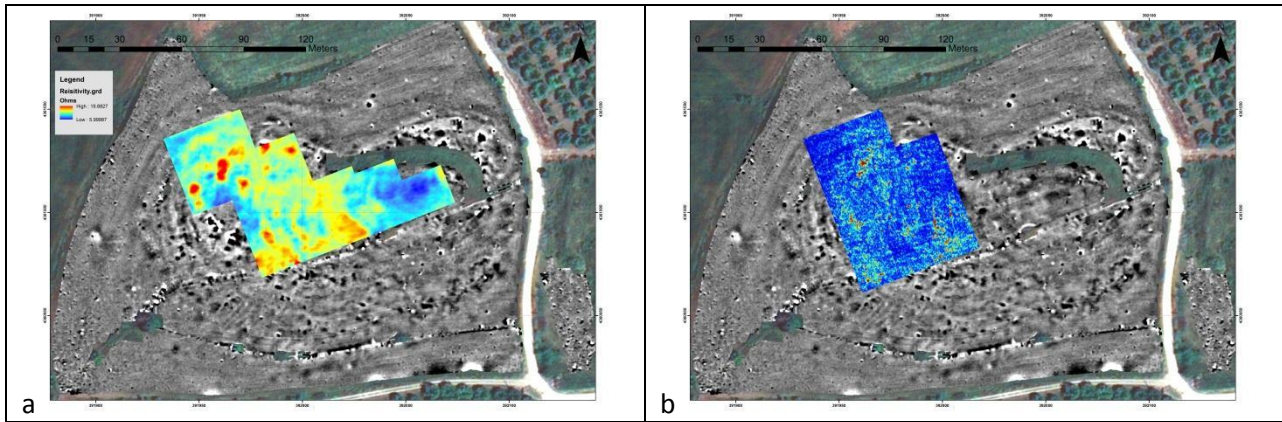


Figure 19: Distribution of geophysical anomalies in relation to each other



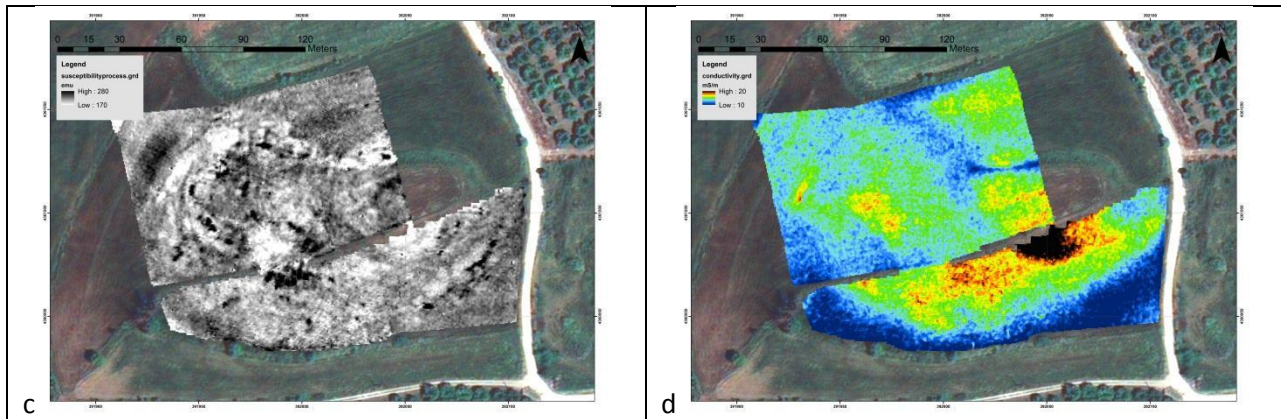


Figure 20: Comparison of a. resistance b. GPR c. susceptibility and d. conductivity results

## Site Bibliography

Grundmann K., 1937. *Magula Hadzimisiotiki*, AM 62, 56-69, πιν. 37, αρ. 8

Halstead P., 1984. *Strategies of survival: an ecological approach to social and economic change in the early farming communities of Thessaly, N. Greece*, Cambridge, (PhD Thesis), 232 (no 8)

Stählin, F. 1924. "Das hellenische Thessalien". Stuttgart., 106

Wace A.J.B. – Thompson M.S., 1912. *Prehistoric Thessaly*, Cambridge. 8, (no. 8)

Αποστολοπούλου - Κακαβογιάννη Ο., 1986. Τοπογραφία της περιοχής των Φερών Θεσσαλίας κατά την προϊστορική περίοδο, *ΑΔ* 34 (1979), 174-206., 180 – 181

Αρβανιτόπουλος, Απ. 1907. "Ανασκαφαί εν Θεσσαλία", Πρακτικά Αρχαιολογικής Εταιρείας, 147 -182. 160

Βουζαξάκης Κ., 2009. *Νεολιθικές θέσεις στη Μαγνησία. Ανασκόπηση – Ανασύνθεση δεδομένων*, στο Αρχαιολογικό Έργο Θεσσαλίας και Στερεάς Ελλάδας 2 (2006), τ. Ι, σελ. 61-74. , 64

Γαλλής Κ., 1992. *Άτλας Προϊστορικών Οικισμών της Ανατολικής Θεσσαλικής Πεδιάδας*, Λάρισα., 103 - 104 (ΑΤΑΕ 271)

Τσουντας Χρ., 1908. *Αι Νεολιθικαί Ακροπόλεις Διμηνίου και Σέσκλου*, Αθήνα., 4 (αρ. 8)